Monatsh Chem (2010) 141:793–800
DOI 10.1007/s00706-010-0330-4

ORIGINAL PAPER

Theoretical conformational analysis of rutin

Paolo Matteini · Andrea Goti · Giovanni Agati

Received: 28 February 2010 / Accepted: 11 May 2010 / Published online: 3 June 2010

Abstract The structural properties of rutin were determined by using a computational multistep progression. In the first step a stochastic strategy based on a molecular mechanics calculation was adopted to obtain a preliminary screening of the low-energy rutin conformations. The most stable structures obtained by the random conformational search were used as a starting point for an Austin Model 1 (AM1) semiempirical optimization. After this treatment, 16 structures characterized by a more stable frontal in respect to back disposition of the glycosidic chain of rutin were identified. To validate the results found from the stochastic search a molecular dynamics simulation was carried out. The results evidenced the presence of a global minimum highly stabilized by a hydrogen bond between the hydroxyl in the 3′ position of the B ring and the endocyclic oxygen of the rhamnose unit followed by approximately 8 kJ mol^{-1} less stable local minima with similar energy values. Finally, the reliability of the molecular model was confirmed by comparing the calculated electronic absorption spectrum with that measured on a methanolic rutin solution.

Keywords Flavonoids · Structure elucidation · Semiempirical calculations · Molecular dynamics

P. Matteini (✉) · G. Agati
Institute of Applied Physics "Nello Carrara",
National Research Council, via Madonna del Piano
10, 50019 Sesto Fiorentino, Italy
e-mail: p.matteini@ifac.cnr.it

A. Goti
Department of Organic Chemistry "Ugo Schiff",
University of Florence, via della Lastruccia 3,
50019 Sesto Fiorentino, Italy

Introduction

Flavonoids constitute a large class of polyphenolic compounds ubiquitous in plants [1], where they play a number of different functions e.g. as attractants to pollinators and seed dispersers, UV screeners and radical scavengers, and defence against bacterial and fungal attack [2–7]. The fundamental structure of flavonoids consists of a γ-benzopyrone (chromone) moiety (rings A and C) to which a benzene ring is linked in the 2 position (B ring) (see Fig. 1 for rutin). All of the three rings can be variably hydroxylated. In vegetables and fruits, flavonoid glycosides having a sugar chain linked to the 3-O position and less frequently to the 7-O position predominate.

As a result of their potentially beneficial impact on human health, the flavonoid quercetin and its glycoside derivatives have progressively come into the focus of medicinal interest [8]. Rutin is considered one of the most promising quercetin derivatives from a biochemical and pharmacological point of view [8, 9]. According to previous studies, rutin has significant anti-inflammatory, antitumour and antioxidant activity as well as vitamin C-sparing action [10], which makes it a popular ingredient of numerous multivitamin preparations and herbal remedies [11, 12]. Furthermore, several other beneficial properties are ascribed to this flavonoid such as an antibacterial and anti-platelet activity, and the capacity to increase the blood vessel elasticity leading to a reduction of haemophilia symptoms [2, 11].

The investigation of the biochemical activity of flavonoids in humans is strictly correlated with the analysis of their interaction with various bioligands, such as proteins, enzymes, vitamins and biopolymers [13]. This problem has been traditionally approached by measuring the changes in the optical or electrochemical properties of the adducts

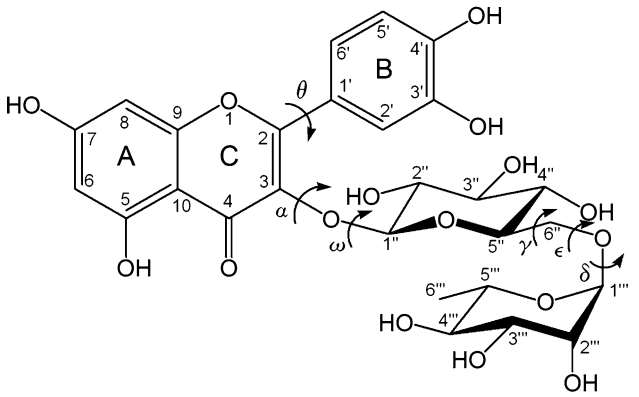

Fig. 1 Representation of the atomic numbering of rutin as used in the text

[14–17], while the insight that the structure of both interacting species may strongly affect the resulting interaction is relatively recent [18–20]. While some data about flavonoid aglycones have appeared in recent years [21–23], the problem of the conformational behaviour of the flavonoid glycosides has been only partially or scarcely treated so far [20, 24, 25].

In a previous study, the molecular structure of quercetin-3-β-glucoside (isoquercitrin) was investigated by means of molecular mechanics and quantum chemical calculations [25]. In this article we aim to extend our insights into quercetin glycosides structuring by focusing on rutin, which has one rhamnose unit linked through the C(6) hydroxyl function of the glucose moiety of isoquercitrin.

The International Union of Pure and Applied Chemistry (IUPAC) numbering of rutin as used in the text is shown in Fig. 1. In rutin 17 rotatable bonds can be counted, but only six of them greatly affect the final conformation energy. They include: θ defined as O(1)C(2)C(1′)C(6′), which indicates the relative position between rings C and B; α and ω defined as C(2)C(3)O(3)C(1″) and C(3)O(3)C(1″)O(1″), which exert control over the orientation of the glycosidic chain; γ defined as O(1″)C(5″)C(6″)O(6″), ε C(5″)C(6″)O-(6″)C(1‴), and δ C(6″)O(6″)C(1‴)O(1‴), which indicate the orientation of the rhamnose with respect to the glucose unit.

Because of the size of the system, ab initio quantum mechanical calculations on rutin are not computationally feasible, since they would require a large basis set in order to obtain reliable information. However, previous works have demonstrated that the combination of molecular mechanics (MM) and Austin Model 1 (AM1) semiempirical method is a relatively fast and accurate choice for determining the structure of flavonoid compounds [21, 25]. In this work we applied a similar strategy to rutin, in order to explore a large number of its conformations within a reasonable time and get an accurate picture of the most stable ones.

Results and discussion

The structural properties of rutin were determined by using a multistep progression due to the complexity of the molecule. In the first step we adopted a stochastic strategy based on an MM calculation to find all minima that are thermodynamically populated. During the search all geometrical parameters were kept relaxed and the values of all torsional angles were collected for each conformation. The random conformational search evidenced the 50 most stable configurations with energy values within 19 kJ mol^{-1} as reported in Table 1. Typically, these structures display values for $\alpha > +60°$ or $\alpha < -60°$ due to the large steric hindrance between the glycosidic chain and the aglycone, which hampers geometries with near co-planarity between the glucose and the benzopyrone moiety. This also leads to α values preferentially associated with ω angles of opposite sign: the $(+\alpha, -\omega)$ pair has the rutinose moiety laying frontally to the chromone part, while $(-\alpha, +\omega)$ angles indicate that the sugar chain lays behind the chromone plane. Concerning the other torsional angles, preferential γ values of approximately $\pm 60°$, dihedral angles ε avoiding the $-60°$ to $+60°$ orientations and negative δ values were collected, which are imposed because of the steric hindrance between the rhamnose and the B ring of the flavonoid.

The 50 low-energy conformations found by MM were used as a starting point for an AM1 semiempirical optimization. After this treatment, we found convergence to 16 stable structures which are listed in Table 2 following a classification into two main groups in accordance with a frontal (10 structures) or a back (6 structures) disposition of the glycosidic chain, that is the $(+\alpha, -\omega)$ and the $(-\alpha, +\omega)$ pairs. The geometrical parameters calculated by the AM1 method are slightly different from those calculated by MM. In particular, we noted that the torsional angles values follow similar criteria and restrictions to those previously found from MM calculations. The observation of the heat of formation values highlights that the lowest energy structures are those where a stabilizing hydrogen bond between the O(4) and the hydroxyl group in the 2″ position of the glucose is established. This hydrogen bond constrains the lone pairs of the oxygen atom of the glucose ring of structures having a $(-\alpha, +\omega)$ pair to be directed toward the B ring, probably resulting in a repulsion effect which accounts for higher formation enthalpy values compared with structures having the sugar in a frontal orientation (i.e. the group with $+\alpha$ and $-\omega$) (Fig. 2; Table 2).

Table 1 Enthalpies and torsional angles of the 50 most stable conformations of rutin obtained by molecular mechanics calculation

	Enthalpy (kJ mol^{-1})	Torsional angles (°)					
		α	ω	γ	ε	δ	θ
1	−30.96	114.73	−40.33	−52.61	176.04	−57.03	−152.87
2	−28.58	−80.61	54.53	−58.37	−161.05	−56.19	153.69
3	−25.02	−81.93	54.59	−58.25	−162.97	−55.13	152.47
4	−24.27	−76.69	65.51	86.00	−84.88	−66.53	−24.26
5	−23.43	105.69	−44.81	82.25	−63.30	−57.67	−152.08
6	−23.22	71.85	−160.89	61.06	170.35	−66.54	27.46
7	−22.64	−70.82	66.72	73.12	−171.75	−58.61	147.39
8	−22.22	116.42	−41.96	−52.82	175.62	−57.02	−152.32
9	−21.55	−76.50	−20.66	74.43	−72.59	−56.26	−25.07
10	−20.04	136.72	−45.37	−56.03	161.26	−64.13	−29.96
11	−19.50	111.16	−49.71	−70.49	69.26	−106.61	−151.96
12	−19.41	−81.10	57.65	−61.83	−164.80	−57.11	−18.66
13	−18.87	−85.13	50.27	−70.49	65.70	−101.82	−19.54
14	−18.49	−78.38	65.21	84.90	−84.54	−65.94	−24.22
15	−18.12	−69.97	71.94	70.18	−174.93	−59.48	−26.48
16	−17.91	107.06	−45.57	−64.37	177.30	−65.52	−151.50
17	−17.91	138.14	−45.43	−56.06	160.97	−63.72	141.45
18	−17.32	−168.32	−173.11	53.59	67.63	−82.83	−29.36
19	−17.03	−67.09	−4.09	−62.60	175.99	−63.81	145.26
20	−16.86	−72.58	61.89	−60.27	−175.96	−158.32	149.55
21	−16.65	84.61	−105.44	−63.40	−160.41	−56.92	23.31
22	−16.40	−77.52	67.54	85.44	−85.88	−66.38	−24.37
23	−16.36	99.69	−100.58	65.28	66.36	−87.18	−153.78
24	−16.23	67.32	−148.64	60.91	171.70	−67.13	27.01
25	−16.19	−79.73	60.17	57.17	160.85	−72.58	−20.59
26	−15.98	−82.11	57.43	−61.24	−166.38	−56.04	−18.70
27	−15.98	109.93	−47.22	82.15	−61.34	−57.04	23.39
28	−15.86	85.89	−55.64	58.84	83.66	−71.64	−144.98
29	−15.52	121.72	−42.38	−52.16	173.35	−57.57	26.56
30	−15.48	−83.38	50.85	−71.25	66.74	−101.65	−18.29
31	−15.40	−83.99	61.02	−69.72	77.56	−100.43	150.77
32	−15.40	−69.09	72.65	62.29	76.82	−77.04	−27.10
33	−15.19	101.43	−99.74	78.26	−83.95	−63.00	−152.52
34	−15.19	166.12	−60.53	−67.22	152.16	−69.36	−34.76
35	−15.15	−69.81	72.07	70.40	−175.02	−58.93	−26.59
36	−15.02	−132.77	168.36	−61.50	178.16	−62.94	146.45
37	−14.43	−88.08	53.70	82.72	−76.96	−59.67	146.30
38	−14.27	−50.30	−55.76	−57.67	162.61	−60.58	−31.32
39	−14.23	−165.81	−171.15	−54.24	171.70	−58.69	37.41
40	−14.18	103.65	−55.53	61.98	176.99	−172.23	−154.03
41	−13.60	132.09	−40.11	−69.98	60.18	176.19	25.67
42	−13.60	−84.81	51.66	−59.01	−179.76	−61.10	14.82
43	−13.22	−77.06	59.64	65.00	75.44	−79.94	144.58
44	−13.14	128.10	−48.54	77.40	−54.76	−53.58	139.13
45	−12.97	−120.19	161.15	−72.10	67.95	−106.82	148.15
46	−12.97	−74.94	77.47	−66.82	−157.39	−53.23	152.99
47	−12.55	−161.89	−175.98	59.78	−95.94	−74.04	−27.55

Table 1 continued

	Enthalpy (kJ mol^{-1})	Torsional angles (°)					
		α	ω	γ	ε	δ	θ
48	−12.47	−85.20	50.17	−70.44	66.02	−102.46	−19.56
49	−12.43	95.32	−54.94	73.82	−87.90	−65.44	−152.10
50	−12.38	97.99	−95.87	61.52	72.74	−81.53	19.23

Table 2 Enthalpies, torsional angles and hydrogen bond lengths of the most stable conformations of rutin obtained by optimization according to the AM1 method

	Enthalpy (kJ mol^{-1})	Torsional angles (°)						Hydrogen bond length (Å)								
		α	ω	γ	ε	δ	θ	H2″–O4	H3′–O1‴	H3′–O2‴	H3′–O4‴	H3′–O3‴	H3′–O6″	H4′–O3‴	H4′–O4‴	H2‴–O4′
Frontal																
Ia	−2,686.38	131.56	−101.26	84.14	−80.03	−67.46	−36.52	2.19	2.16							
Ib	−2,677.59	117.41	−98.07	76.72	−110.02	−68.58	−137.95	2.20								
Ic	−2,677.43	113.78	−101.15	78.53	70.84	−97.14	−133.49	2.15			2.15					
Id	−2,671.02	120.25	−98.41	69.14	169.36	−98.73	−140.63	2.19				2.15				
IIa	−2,679.43	120.94	−97.93	−70.72	−101.72	−77.37	−38.37	2.21					2.20			
IIb	−2,675.38	108.07	−99.05	−77.81	−133.67	−62.50	17.04	2.16					2.26		2.26	
IIIa	−2,677.72	90.47	−144.93	75.60	148.31	−73.97	22.26	2.20					2.19	2.29		
IIIb	−2,675.84	77.21	−148.24	70.81	171.69	−67.13	−27.00	2.21					2.21			
IVa	−2,672.11	130.13	−75.38	81.11	−87.10	−75.96	147.00									
IVb	−2,669.89	124.87	−68.58	74.88	−171.48	−63.09	−141.15					2.16				
Back																
	−2,673.70	−100.98	63.16	72.22	87.69	−78.62	−30.76	2.11						2.76		
	−2,672.11	−101.15	54.87	−57.59	−150.01	−62.48	142.48	2.15			2.14					
	−2,666.55	−102.31	61.83	−80.46	77.94	−120.25	140.36	2.09		2.31						
	−2,661.36	−102.50	55.65	−74.95	−173.28	−94.47	88.09	2.13	2.16							
	−2,667.97	−136.49	156.14	59.59	−93.55	−75.14	−37.49			2.15						
	−2,662.36	−130.89	159.99	−73.19	70.34	−109.93	144.82									2.74

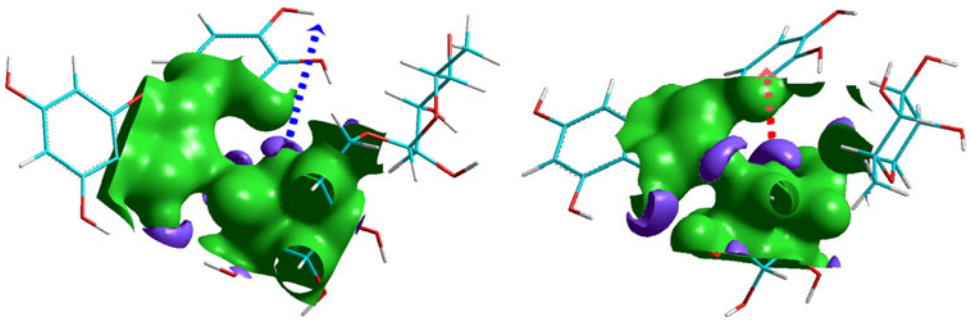

Fig. 2 Comparison between rutin conformers having a frontal (*left*) or a back (*right*) disposition of the sugar chain. In the latter the lone pairs of the O(1″) and the B ring of the chromone are in close proximity, which is supposed to decrease the stability of the system. *Dashed arrows* indicate the axis of the lone pairs

This latter group was further organized into four subgroups (**I**–**IV**) accounting for similar groupings of ω and γ values (Table 2). We may note that the conformations within the four subgroups differ in the type of hydrogen bonds formed between the sugar chain and the hydroxyl groups of the B ring, which in turn affect the energy order of the different forms. The subgroup **I** is the most populated and contains the global minimum (**Ia**, Fig. 3). The latter

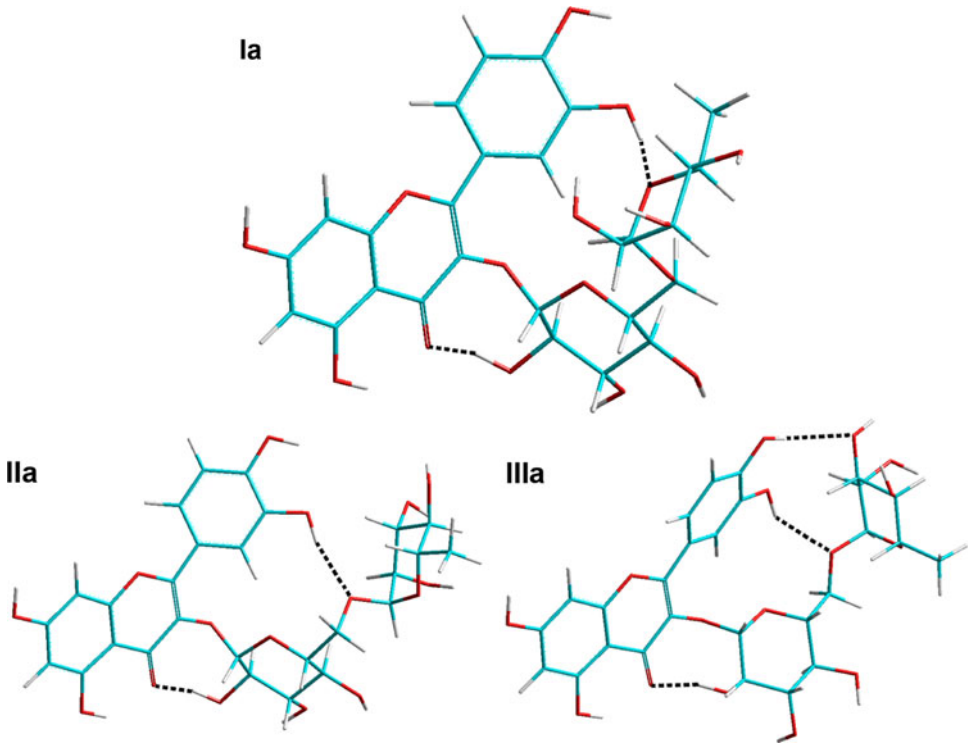

Fig. 3 Representation of the three most stable conformations of rutin found after energy minimization (**Ia**, **IIa** and **IIIa**). The hydrogen bonds formed between the chromone and the sugar units are represented by *dashed lines*

shows a minimum of 8 kJ mol^{-1} difference with respect to the other conformations of its subgroup and of the other groups, which has to be ascribed to a twisted conformation that ensures the formation of a favourable hydrogen bond between the endocyclic O(1‴) and the H(3′). The subgroups **II** and **III** show a more unfolded (open) arrangement characterized by the establishment of a hydrogen bond between the hydroxyl in the 3′ position of the B ring and the oxygen connecting the two sugar units (O(6″)) (Fig. 3). This, in spite of inducing a certain stabilization, actually hinders a favourable alignment of the hydrogen bond established between the H(2″) and the carbonyl group of the chromone as observed in the **Ia** conformer. The lack of this latter hydrogen bond is instead probably responsible for the higher enthalpies observed for the group **IV** members.

To validate the results of the stochastic search, a molecular dynamics (MD) simulation, followed by an energy minimization, was carried out. The simulation consisted in annealing the system at a given temperature in the 100- to 300-K range followed by cooling down to 0 K. For example, Fig. 4 displays the evolution of the torsional angles ε, δ and θ as a function of the simulation time for conformation **Ib** with fixed α (125°), ω (−100°) and γ (75°) torsional angles using a 300 K simulation temperature. On performing the simulation on each member of the **I** subgroup, no new minima were found. Moreover, the local minima **Ib**, **Ic** and **Id** converged to conformation **Ia**. Similar calculations were performed on the most stable conformers of the **II** and **III** subgroups (i.e. **IIa** and **IIIa**),

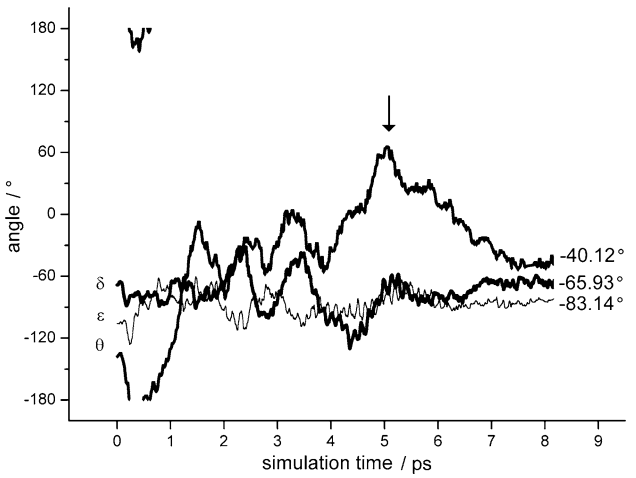

Fig. 4 Evolution of the ε, δ and θ torsional angles of the **Ib** conformer during a molecular dynamics simulation. The simulation included: a heating time = 0.1 ps starting from $T = 0$ K; an annealing time = 5 ps at a constant $T = 300$ K; a cooling time = 3 ps (onset indicated by an *arrow*) down to $T = 0$ K. The final values of the torsional angles are indicated on the *right*

obtaining final unmodified enthalpy values, to which the lower energy subgroup members (**IIb** and **IIIb**) converged upon annealing. These results confirmed the presence of a highly stabilized global minimum (**Ia**) preferentially populated at room temperature and followed by two local minima (**IIa** and **IIIa**) with similar enthalpy values (Fig. 3). Less stable conformations are instead those lacking a H(2″)–O(4) bond or having a back disposition of the

Table 3 Calculated bond lengths, bond angles and dihedral angles of the conformation **Ia** of rutin

	Bond length (Å)		Bond angles (°)		Dihedral angles (°)
O1–C2	1.39	C9–O1–C2	118.85	C3′–C4′–O4′–H4′	−0.79
O1–C9	1.38	O1–C2–C3	121.45	C2′–C3′–O3′–H3′	−22.28
C2–C3	1.37	C2–C3–C4	122.22	C2–C3–O3–C1″ = α	131.56
C3–C4	1.47	C3–C4–C10	115.04	C3–O3–C1″–O1″ = ω	−101.26
C4–C10	1.46	C4–C10–C9	119.18	C6–C5–O5–H5	178.30
C5–C10	1.42	C4–C10–C5	123.46	C8–C7–O7–H7	−0.32
C5–C6	1.40	C10–C5–C6	121.15	O1–C2–C1′–C6′ = θ	−36.52
C6–C7	1.40	C5–C6–C7	119.10	C2–C3–C4–O4	173.86
C7–C8	1.40	C6–C7–C8	121.70	O1–C2–C3–O3	173.44
C8–C9	1.40	C7–C8–C9	117.89	C9–O1–C2–C1′	179.20
C9–C10	1.41	C8–C9–C10	122.81	C10–C4–C3–O3	−176.36
C2–C1′	1.46	C3–C2–C1′	128.63	C4–C3–C2–C1′	−173.85
C1′–C2′	1.40	C2–C1′–C6′	119.50	O1″–C5″–C6″–O6″ = γ	84.14
C2′–C3′	1.40	C6′–C5′–C4′	119.57	C5″–C6″–O6″–C1‴ = ε	−80.03
C3′–C4′	1.41	C5′–C4′–C3′	119.65	C6″–O6″–C1‴–O1‴ = δ	−67.46
C4′–C5′	1.40	C4′–C3′–C2′	120.57		
C5′–C6′	1.39	C3′–C2′–C1′	119.37		
C6′–C1′	1.40	C2′–C1′–C6′	120.04		
C4–O4	1.25	C2–C3–O3	119.17		
C5–O5	1.36	C4–C3–O3	117.99		
C7–O7	1.37	C3–C4–O4	121.53		
C3′–O3′	1.38	C10–C4–O4	123.43		
C4′–O4′	1.37	C10–C5–O5	124.27		
		C6–C5–O5	114.58		
		C6–C7–O7	116.29		
		C8–C7–O7	122.01		
		C2′–C3′–O3′	123.20		
		C4′–C3′–O3′	116.23		
		C3′–C4′–O4′	122.72		
		C5′–C4′–O4′	117.63		

sugar chain, as just previously pointed out. The bond lengths, the bond angles and the most important torsion angles of the fully optimized conformation **Ia** are summarized in Table 3. The calculated values are mostly comparable with those previously reported for the isoquercitrin molecule [25], with the exception of the C(2′)C(3′)O(3′)H(3′) dihedral angle, which has to be ascribed to the presence of the stabilizing hydrogen bond between the B ring and the rhamnose unit (absent in the isoquercitrin molecule).

We finally compared the experimental absorption spectrum of rutin with that theoretically calculated by a configuration interaction (CI) calculation on the AM1 optimized structure (see Fig. 5). Comparable theoretical spectra were obtained for **Ia**, **IIa** and **IIIa** structures. The theoretical frequencies are in good agreement with those of the exper-

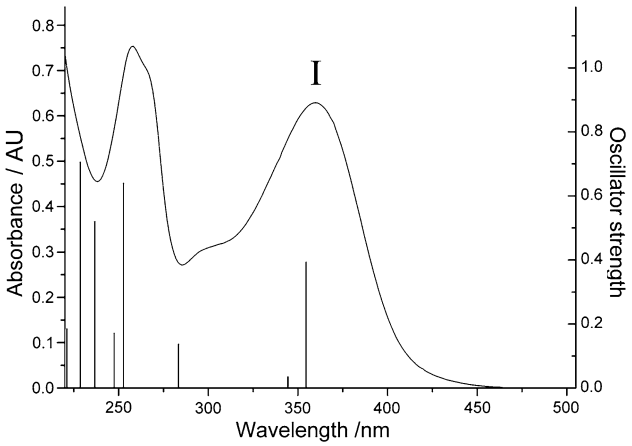

Fig. 5 Comparison of the experimental and calculated electronic spectra of rutin

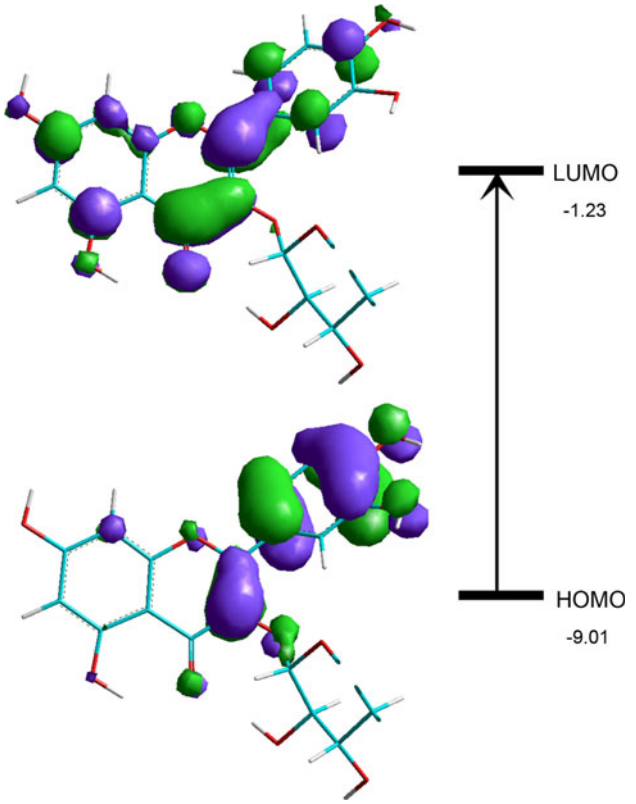

Fig. 6 Frontier orbital shapes mainly involved in the transition corresponding to the band I in the electronic spectrum of rutin. The rhamnose moiety is omitted for clarity. Energy levels are expressed in electronvolts (eV)

imental spectrum. The slight blue shift of the calculated band I ($\lambda = 355$ nm) with respect to the experimental value ($\lambda_{max} = 359$ nm) and other slight discrepancies between the calculated and the experimental spectra are likely to be ascribed to the presence of the solvent. Moreover, agreement was found between the line heights of the calculated spectrum which are relative to the value of oscillator strengths, and the experimental absorption coefficients. The frontier molecular orbitals calculated for the **Ia** conformer are depicted in Fig. 6. These show a pronounced π character with no participation of the sugar chain. Band I is mainly assigned to the HOMO–LUMO transition and is characterized by a charge transfer from the B ring to the chromone portion of the molecule and in particular to the carbonyl group. The agreement between the calculated and the experimental electronic spectra of rutin supports the reliability of the theoretical model used.

Conclusions

In this investigation a combination of MM and AM1 semiempirical calculations was exploited to find the most stable conformations of isolated rutin. The structural characteristics of stable conformers were validated by MD simulation. The calculations evidenced three stable minima differing in the type of hydrogen bonds formed between the B ring and the rhamnose unit, with the most favoured showing a bond between the OH(3′) and the endocyclic oxygen in 1‴. Finally, the good agreement between the experimental electronic absorption spectrum and those calculated for the three minimum conformations testifies to the solidity of the proposed modelization.

Future work will be devoted to the investigation of the behaviour of rutin when passing from an in vacuo to an aqueous environment. In fact the conformation of rutin is expected to be potentially influenced by the presence of water, which may interact with a number of OH groups throughout the molecule by formation of hydrogen bonds. Such bonds, at least at an intramolecular level, have been shown to play a main role in the molecular structuring of rutin as clearly evidenced by this study.

Methods

We first applied an MM calculation [26] to obtain a preliminary screening of the low-energy rutin conformations. This method appeared the most convenient to perform due to the extensive computations required by the complexity of the examined flavonoid molecule. We carried out a conformational search based on a stochastic approach using the AMBER [27] potential energy function setup with a root mean square (RMS) gradient of 0.004 kJ mol^{-1} and using a termination criterion of 10,000 iterations. The method involves a random variation of the main dihedral angles (α, ω, γ, ε, δ and θ) to generate new structures and then energy minimizing each of those. Low-energy unique conformations are stored while high-energy or duplicate structures are discarded. Then, to improve the structure optimization, an AM1 [28] geometrical optimization was carried out on the most stable conformations found by MM. The AM1 method has the advantage of taking into account the hydrogen bonding, which is a fundamental interaction for flavonoid molecules [29]. Moreover, compared with other semiempirical methods such as the modified neglect of diatomic overlap (MNDO) method, it does not overestimate the repulsion between atoms separated by distances approximately equal to the sum of their van der Waals radii [28]. The energy minimization was run by using the Polak–Ribière algorithm with a convergence criterion of 0.004 kJ mol^{-1}. Furthermore a molecular dynamics simulation [30], using the AM1 force field, was performed to assess that the lowest energy structure observed corresponded to a global minimum and to surmount possible energy barriers among most stable conformers. In this step

all geometrical parameters were relaxed except for the torsional angles α, ω and γ, whose values served to fix the orientation of the glucose unit. A typical molecular dynamics run included a heating time of 0.1 ps starting from 0 K, a 5- to 10-ps time at a constant temperature fixed in the 100- to 300-K range and a 3-ps cooling time to come back to 0 K. After the simulation, an AM1 geometrical optimization was performed to refine the obtained structures.

Finally the electron absorption spectra of the most stable conformers were calculated by using a configuration interaction (CI) treatment [31]. This calculation accounted for the contribution of singly excited configurations involving the nine highest occupied and the nine lowest unoccupied molecular orbitals.

All the calculations were performed with the Hyperchem (version 7.5) software on a Pentium 4 3.20 GHz computer.

The UV–Vis absorption spectrum of rutin (Extrasynthèse, Lyon-Nord, Genay, France) in methanol (at a concentration of 5×10^{-5} mol dm^{-3}) was recorded with a Jasco 560 V UV–Vis spectrophotometer (Jasco, Tokyo, Japan) using 1-cm-path-length cells.

References

1. Harborne JB (1994) The Flavonoids: advances in research since 1986. Chapman and Hall, London
2. Harborne JB, Williams CA (2000) Phytochemistry 55:481
3. Dixon RA, Paiva NL (1995) Plant Cell 7:1085
4. Reuber S, Bornman JF, Weissenböck G (1996) Physiol Plant 97:160
5. Pfündel EE, Agati G, Cerovic ZG (2006) Optical properties of plant surfaces. In: Riederer M, Müller C (eds) Biology of the plant cuticle. Annu Plant Rev, vol 23. Blackwell, Oxford, p 215
6. Hernández I, Alegre L, Van Breusegem F, Munné-Bosch S (2009) Trends Plant Sci 14:125
7. Agati G, Matteini P, Goti A, Tattini M (2007) New Phytol 174:77
8. Ren W, Qiao Z, Wang H, Zhu L, Zhang L (2003) Med Res Rev 23:519
9. Wang HK (2000) Expert Opin Investig Drugs 9:2103
10. Rice-Evans CA, Miller NJ, Paganga G (1997) Trends Plant Sci 2:152
11. Cushnie TP, Lamb AJ (2005) Int J Antimicrob Agents 26:343
12. Havsteen BH (2002) Pharmacol Ther 96:67
13. Cody V, Middleton E, Harborne JB (1985) Plants flavonoids in biology and medicine: biochemical, pharmacological, and structure-activity relatioships. Alan R Liss, New York
14. Xi J, Guo R (2007) Int J Biol Macromol 40:305
15. Kanakis CD, Tarantilis PA, Polissiou MG, Diamantoglou S, Tajmir-Riahi HA (2006) J Mol Struct 798:69
16. Hodek P, Hanustiak P, Krízková J, Mikelova R, Krízková S, Stiborová M, Trnková L, Horna A, Beklová M, Kizek R (2006) Neuro Endocrinol Lett 27(Suppl 2):14
17. Papadopoulou A, Green RJ, Frazier RA (2005) J Agric Food Chem 2005:158
18. Zsila F, Bikádi Z, Simonyi M (2006) Biochem Pharmacol 65:447
19. Lin CM, Chen CS, Chen CT, Liang YC, Lin JK (2002) Biochem Biophys Res Commun 294:167
20. De Oliveira EB, Humeau C, Chebil L, Maia ER, Dehez F, Maigret B, Ghoul M, Engasser J-M (2009) J Mol Catal B Enzym 59:96
21. Cornard JP, Merlin JC, Boudet AC, Vrielynck L (1997) Biospec 3:183
22. Russo N, Toscano M, Uccella N (2000) J Agric Food Chem 48:3232
23. Amat A, De Angelis F, Sgamellotti A, Fantacci A (2008) J Mol Struct 868:12
24. Mielczarek C (2005) Eur J Pharm Sci 25:273
25. Cornard JP, Boudet AC, Merlin JC (1999) J Mol Struct 508:37
26. Allinger NL (1977) J Am Chem Soc 99:8127
27. Cornell WD, Cieplak P, Bayly CI, Gould IR, Merz KM Jr, Ferguson DM, Spellmeyer DC, Fox T, Caldwell JW, Kollman PA (1995) J Am Chem Soc 117:5179
28. Dewar MJS, Zoebisch EG, Healy EF, Stewart JJP (1985) J Am Chem Soc 107:3902
29. Dannenberg JJ, Evleth EM (1992) Int J Quant Chem 44:869
30. Karplus M (2003) Biopolymers 68:350
31. Sherrill CD, Schaefer HF III (1999) Adv Quant Chem 34:143